

IBM Research Report

Minor Alloying Effects of Ni or Zn on Microstructure and Microhardness of Pb-free Solders

Sun-Kyoung Seo, Moon Gi Cho

Samsung Electronics
San#24 Nongseo-Dong
Giheung-Gu, Yongin-City
Gyeonggi-Do 446-711
Republic of Korea

Sung K. Kang

IBM Research Division
Thomas J. Watson Research Center
P.O. Box 218
Yorktown Heights, NY 10598
USA

Jaewon Chang, Hyuck Mo Lee

Department of Materials Science and Engineering
KAIST
335 Gwahangno, Yuseong-gu
Daejeon 305-701
Republic of Korea



Research Division

Almaden - Austin - Beijing - Cambridge - Haifa - India - T. J. Watson - Tokyo - Zurich

Minor Alloying Effects of Ni or Zn on Microstructure and Microhardness of Pb-free Solders

Sun-Kyoung Seo^{1*}, Moon Gi Cho¹,
Sung K. Kang²,
Jeawon Chang³, and Hyuck Mo Lee³

1. Samsung Electronics, San#24 Nongseo-Dong, Giheung-Gu, Yongin-City, Gyeonggi-Do 446-711, Republic of Korea

2. IBM T.J. Watson Research Center, Yorktown Heights, New York 10598

3. Department of Materials Science and Engineering, KAIST, 335 Gwahangno,
Yuseong-gu, Daejeon 305-701, Republic of Korea

* E-mail: sk1050.seo@samsung.com

Abstract

To form reliable Pb-free solder joints, minor alloying additions of Ni or Zn to Sn-rich solders have been recommended recently. Several beneficial effects of Ni or Zn minor alloying additions to Pb-free solders were reported to improve solder joint reliability. But the effects of Ni or Zn minor alloying additions on the bulk properties of solders are not systematically evaluated in light of understanding the electromigration or mechanical reliability of solder joints. Therefore, in this study, the minor alloying effects of Ni or Zn on the microstructure and microhardness in terms of Ni or Zn composition and cooling rate are investigated. The amounts of minor alloying elements investigated are in the range of 0.05-0.15 wt% for Ni, and 0.2-0.6wt% for Zn, which cover the reported composition ranges to enhance solder/UBM joint reliability. Three cooling rates are employed during solidification; 0.02 °C/s (furnace-cooling), about 5 °C/s (air-cooling), and 100 °C/s or higher (quenching). The microstructure of Ni or Zn doped solders is evaluated in terms of composition, undercooling during solidification, and cooling rate. The phase diagram analysis is conducted to explain the microstructural variations. The microstructures of Ni or Zn doped solders are well correlated to their microhardness data.

Introduction

Extensive research on Pb-free solders has recently recognized the near-eutectic Sn-Ag-Cu solder alloys as a most promising candidate for consumer electronics, such as surface-mount card assembly for BGA (ball grid array) solder joints. However, there are still several problems to be solved in applying these Pb-free solders for more challenging applications. For example, in Sn-Ag or Sn-Ag-Cu, large Ag₃Sn plates formed in the solder matrix can facilitate fatigue crack initiation and propagation, reducing the life time of solder joints. In addition, the formation of Cu₃Sn layer at the interface between Sn-rich solders and a Cu substrate during a long-time aging can induce Kirkendall-type voids at the interface and thereby degrade the drop impact resistance of Pb-free solder joints [1-3].

In order to produce more reliable Pb-free solder joints, minor alloying additions of various elements to Sn-rich solders have been extensively investigated recently. Among them, a minor amount of Ni or Zn was found to be most effective in controlling the interfacial reactions with Cu

UBMs, by reducing Cu₃Sn formation, consumption of Cu UBM, and interfacial void formation [2, 3]. However, the previous studies have mainly focused on the interfacial reactions between Pb-free solders and Cu or Ni UBM. No information is available on the modification of bulk properties due to the minor alloying additions, such as the microstructures and mechanical properties.

In this study, it is investigated the effects of the Ni or Zn minor elements on the microstructure of Sn-rich solders and their mechanical properties. Because Sn-rich solders consist of mostly Sn, it is expected that the Sn crystal structure (bct) and anisotropic properties would significantly affect the microstructure of Pb-free solder joints, and thereby their mechanical and electromigration properties [4-6]. Another important factor affecting the mechanical properties of solder joints is the characteristics of intermetallics formed in a solder matrix (type, size, density and distribution of intermetallic compounds). Therefore, the microstructure (Sn grains, orientation, and IMC characteristics) and microhardness of Ni or Zn doped solders are characterized as functions of alloy composition and cooling rate in this study.

Experimental procedures

The solder compositions investigated in this study are Sn-1.8Ag-xNi (x: 0, 0.05, 0.10 and 0.15 wt %) and Sn-1.0Ag-xZn (x: 0, 0.2, 0.4, and 0.6 wt%). The solders used are in the form of solder balls (380 μm in diameter), which were commercially produced. As-received solder balls were rapidly solidified or quenched at a cooling rate of about 100 °C/sec or higher during their production by the supplier. The as-received solder balls were first reflowed at 250 °C for 10 min in a vacuum oven and then cooled either in air (~5 °C/sec) or in a furnace (~0.02 °C/sec). Some solder balls were reflowed on a PCB substrate and then cooled down in air. The PCB substrate has Cu OSP finish with an open pad size of 300 μm in diameter.

The reflowed solder joints and bulk solder balls were cross-sectioned, fine-polished and examined with an optical microscope under cross-polarized imaging conditions. Optical cross-polarization imaging technique has been extensively demonstrated as a useful tool to evaluate the Sn grain size [4-9]. To obtain the information on grain size and β-Sn crystal orientation, electron backscatter diffraction (EBSD) technique was further employed. Information about the crystal orientation of β-Sn grains is displayed perpendicular to the substrate, namely, parallel to the cooling direction. The cross-

sectioned samples are mapped and analyzed with the vertical reference direction (RD) \parallel [100].

Subsequently, the DSC (differential scanning calorimetry) technique was used to measure the undercooling of the solder alloys. The solder samples were heated and cooled at a rate of 6 °C/min under a nitrogen atmosphere. One solder ball (380 μ m, 0.01 mg) was used in a DSC run to eliminate possible occurrence of multiple peaks during the solidification process. In addition, the onset temperatures reported in this study are the average values of DSC results obtained with five samples of each solder.

For thermodynamic calculations, the Thermo-Calc software was used. And, the microhardness tests were performed using 5 g force and 5 s dwell-time on the cross-sectioned surface of solder balls. The Vickers hardness number (VHN) was reported as an average value by measuring 15 indentations or more.

Results and Discussion

Ni minor alloying effect on the microstructure of Sn-Ag solder

Figure 1 shows a collection of cross-polarized images of Sn-Ag-Ni solders as a function of Ni composition and cooling rate. Sn-1.8Ag solders have fine 60 degree twins in 380 μ m diameter ball as reported previously [8, 9]. And, as the cooling rate increases, twins in Sn-Ag become finer. In the quenched, all Sn-Ag-Ni solders show also fine twins similar to Sn-Ag. However, in the air-cooled, twins become somewhat larger than in the quenched for SA-0.05Ni and SA-0.10Ni, while one or two large grains are usually observed in SA-0.15Ni air-cooled. In addition, the number of grains decreases in the furnace-cooled solders, producing a single grain structure as the Ni content increases.

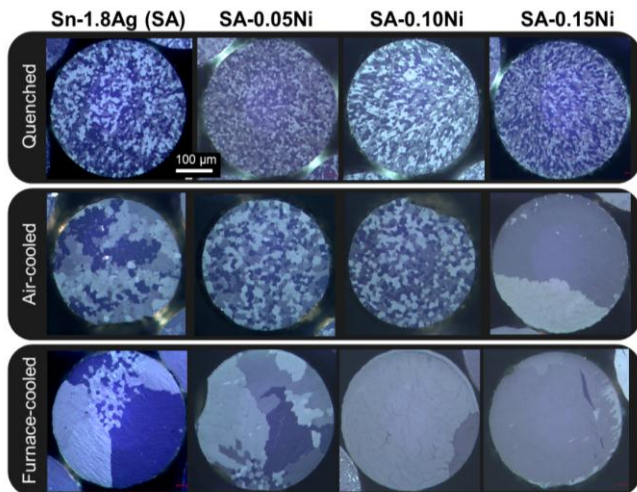


Figure 1. Cross-polarized images of Sn-1.8Ag-Ni solder balls as a function of cooling rate and Ni composition (0 wt%, 0.05 wt%, 0.10 wt%, and 0.15 wt%).

SEM images of Fig 2, reveal the microstructure of air-cooled Sn-Ag-Ni where a drastic increase of grain size is

observed. Sn-Ag, SA-0.05Ni, and SA-0.10Ni show fine twins all over, small β -Sn dendrites and IMC particles along the dendrite boundaries as shown in Fig 2(a), 2(b), and 2(c). In contrast, large β -Sn dendrites and eutectic area are observed in SA-0.15Ni, Fig 2(d). The addition of 0.15% Ni to Sn-1.8Ag is found to be quite effective to coarsen the microstructure.

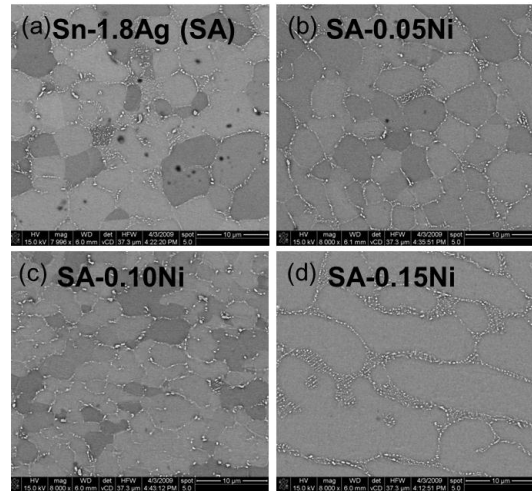


Figure 2. SEM images of Sn-1.8Ag-Ni solders air-cooled.

Table 1. DSC results for undercooling of Sn-Ag-Ni solders.

Solder (wt%)	Onset temperature (°C)		Undercooling (T1-T2)
	Heating (T1)	Cooling (T2)	
Sn-1.8Ag	223.4	172.6	50.8
Sn-1.8Ag-0.05Ni	222.9	178.0	44.9
Sn-1.8Ag-0.10Ni	222.7	178.5	44.2
Sn-1.8Ag-0.15Ni	222.7	206.8	15.9

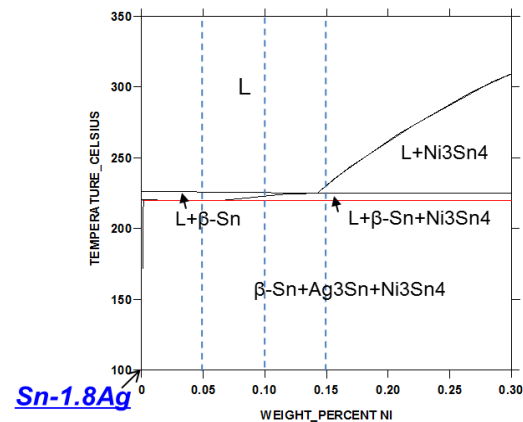


Figure 3. The Sn-rich region of the calculated ternary Sn-Ag-Ni phase diagram.

Table 1 illustrates the DSC results of melting and solidification temperatures of Sn-1.8Ag-xNi. The amount of the undercooling is estimated for each solder composition. The undercooling of Sn-1.8Ag is about 50 °C. And the amount of the undercooling steadily decreases as the Ni content increases. The undercooling is reduced to about 15 °C for SA-0.15Ni. This could be related to the microstructure coarsening shown in Sn-Ag-0.15Ni of Fig 1 and Fig 2.

Referring to the previous study on the microstructure of Sn-Cu-Zn/Ni joints [10], there is a tendency that a smaller undercooling tends to coarsen β -Sn dendrites. Furthermore, as noted in the phase diagram of Fig 3, Sn-1.8Ag-0.15Ni has a higher liquidus temperature and the Ni_3Sn_4 phase as a primary phase, which is different from other Sn-Ag-Ni alloys with Ni less than 0.15 wt%. In summary, Sn-Ag-0.15Ni is found to be a critical composition which affects the undercooling, liquidus temperature, and primary phase, all inducing the microstructure coarsening.

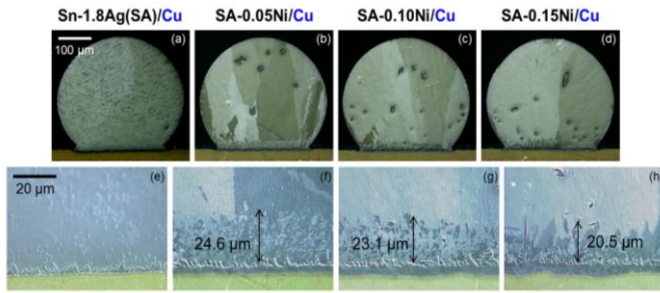


Figure 4. Cross-polarized images of Sn-Ag-Ni/Cu UBM joints; (a)-(d) images for whole solder joints and (e)-(h) enlarged images for solder/Cu interface.

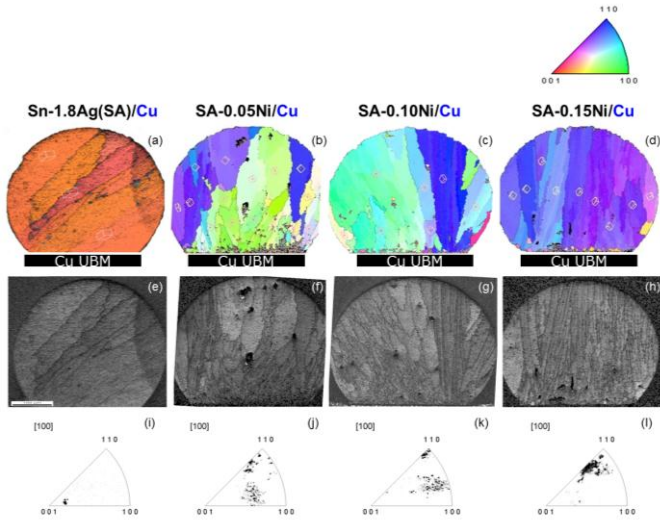


Figure 5. EBSD results of Sn-Ag-Ni/Cu UBM joints; (a)-(d) inverse pole figure maps, (e)-(h) image quality maps, and (i)-(l) inverse pole figures.

When a Sn-rich solder is joined to Cu UBM, Cu atoms dissolve into the liquid solder and change the microstructure of the solder during reflow. As previously reported, Sn-Ag solder changes to a Sn-Ag-Cu ternary alloy by the dissolution of about 1.0 wt% of Cu and this often produces a few large grains having near [001] direction instead of fine twins of Sn-Ag [11]. However, there are significant differences in the microstructure between Sn-Ag/Cu joint and Sn-Ag-Ni/Cu joint as shown in Fig 4 and Fig 5. In all Sn-Ag-Ni/Cu joints, columnar grains having near [110] and [100] directions are observed as shown in Fig 5. The columnar grains having near [110] and [100] directions were also observed in most Sn-Cu/Cu joints [11]. However, at the Sn-Ag-Ni/Cu interface,

fine grains are observed as shown in Fig 4(f)-4(h). The thickness of this fine grain area is over than 20 μm . The EBSD result of Fig 6 demonstrates that the fine grains are cyclic twins having 60 degree angle. Fine twins near the Sn-Ag-Ni/Cu interface might be caused due to a higher Ag composition near the interface.

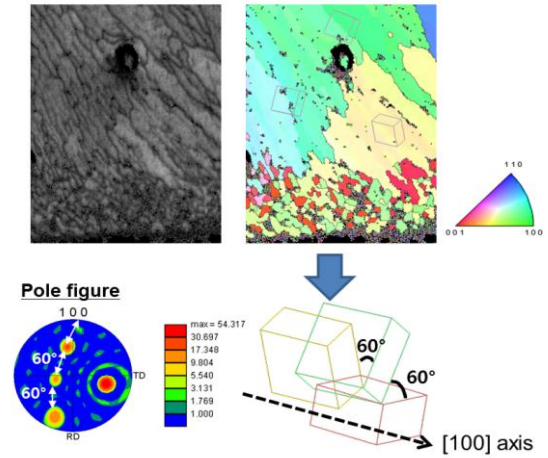


Figure 6. EBSD results of Sn-1.8Ag-0.1Ni/Cu UBM joint interface.

The interfacial IMC in Sn-Ag-Ni/Cu joint is thicker than in Sn-Ag/Cu joint. As the amount of Ni content increases, the interfacial IMC thickness increases gradually. The interfacial IMCs of Sn-Ag/Cu and Sn-Ag-Ni/Cu joints are confirmed to be Cu_6Sn_5 and $(\text{Cu,Ni})_6\text{Sn}_5$ respectively, which is consistent with the previous reports [6, 12].

Another difference in the microstructure between Sn-Ag-Ni/Cu and Sn-Ag/Cu is that there are several $(\text{Cu,Ni})_6\text{Sn}_5$ primary phases in Sn-Ag-Ni/Cu joints. Judging from the compositional analysis, the dissolution of Cu to solder in Sn-Ag-Ni/Cu joint is expected to be the same as in Sn-Ag/Cu joint, about 1.0 wt% during reflow [11]. The Cu dissolution of 1.0 wt% in Sn-Ag-Ni/Cu joint would make the solder composition be in the $\text{L}+\text{Cu}_6\text{Sn}_5$ coexisting area as shown in the Sn-Ag-Cu-Ni quaternary phase diagram of Fig 7. This would induce more the primary Cu_6Sn_5 phase than in the Sn-Ag/Cu joint during cooling.

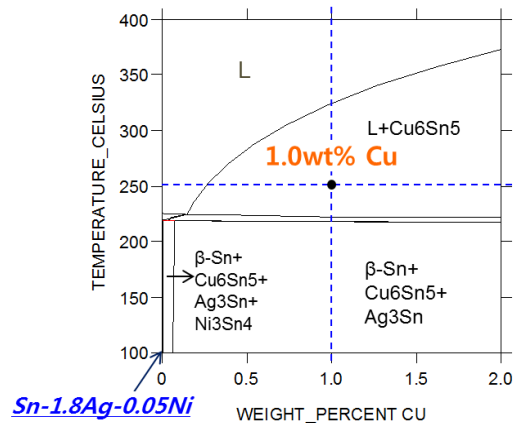


Figure 7. The Sn-rich region of the calculated quaternary Sn-1.8Ag-0.05Ni-Cu phase diagram.

Zn minor alloying effect on the microstructure of Sn-Ag solder

Figure 8 shows cross-polarized images of Sn-Ag-Zn solders as a function of cooling rate and Zn composition. Comparing the microstructure of Sn-Ag to Sn-Ag-Zn in Fig 8, β -Sn grain orientation and dendrite cell size are similar each other in the air-cooled condition. But they are significantly different from each other in the quenched and furnace-cooled conditions. In the quenched, several large grains together with fine twins are locally observed in Sn-Ag-Zn, while only fine twins are noticed in Sn-Ag. In the furnace-cooled, Sn-Ag-Zn shows only beach-ball shaped large cyclic twins, not fine twins. In addition, it is also observed that the β -Sn dendrites in Sn-Ag-Zn are much larger than Sn-Ag, and the coarsened IMC particles are observed along the dendritic boundaries.

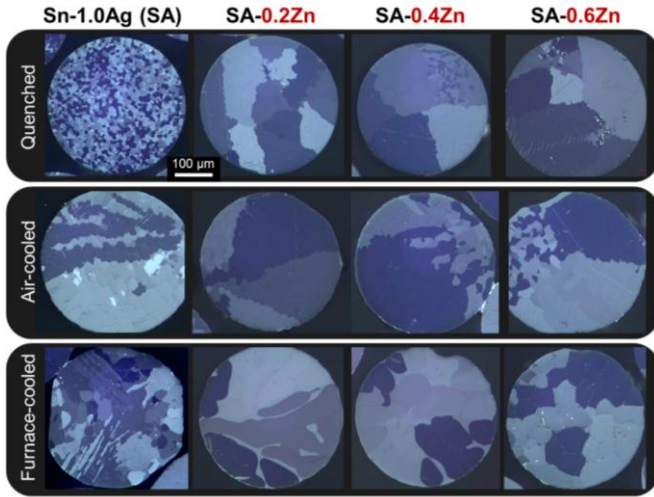


Figure 8. Cross-polarized images of Sn-1.0Ag-Zn solder balls as a function of cooling rate and Zn composition (0 wt%, 0.2 wt%, 0.4 wt%, and 0.6 wt%).

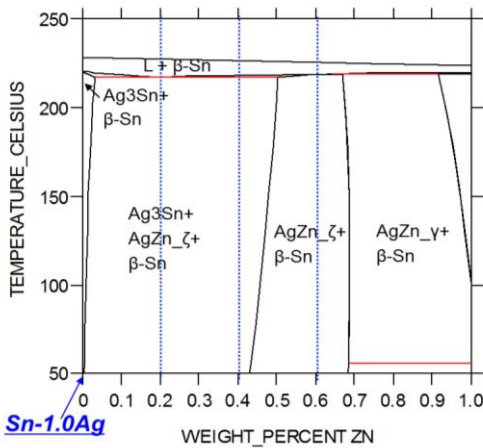


Figure 9. The Sn-rich region of the calculated ternary Sn-1.0Ag-Zn phase diagram.

From the ternary phase diagram of Sn-Ag-Zn, Fig 9, it is recognized that the addition of 0.2, 0.4, and 0.6 wt% Zn into Sn-1.0Ag would facilitate the formation of AgZn- ζ phase besides Ag₃Sn in Sn matrix. The amount of Ag₃Sn and AgZn- ζ

IMCs could be compared by calculating the mole percent of each phase in the equilibrium state at 150 °C as shown in Table 2. As the amount of Zn doping in Sn-Ag-Zn increases from 0 to 0.6 wt%, the mole % of Ag₃Sn phase decreases while the mole % of AgZn- ζ phase increases, and finally only AgZn- ζ phase is formed in Sn-1.0Ag-0.6Zn. The reduction of Ag₃Sn particles appears to induce a few large grains instead of fine twins in Sn-Ag-Zn.

Table 2. The calculated equilibrium phases at 150 °C and their mole percent in Sn-1.0Ag-Zn ternary system.

Solder composition	Equilibrium phases at 150°C and their mole percent
Sn-1.0Ag	β -Sn (98.57%), Ag ₃ Sn (1.43%)
Sn-1.0Ag-0.2Zn	β -Sn (98.38%), Ag ₃ Sn (0.86%), AgZn- ζ (0.77%)
Sn-1.0Ag-0.4Zn	β -Sn (98.17%), Ag ₃ Sn (0.24%), AgZn- ζ (1.59%)
Sn-1.0Ag-0.6Zn	β -Sn (97.89%), AgZn- ζ (2.11%)

Table 3. DSC results for undercooling of Sn-Ag-Zn solders.

Solder (wt%)	Onset temperature (°C)		Undercooling (T1-T2)
	Heating (T1)	Cooling (T2)	
Sn-1.0Ag	224.3	191.5	32.8
Sn-1.0Ag-0.2Zn	219.6	216.1	3.5
Sn-1.0Ag-0.4Zn	219.1	217.1	2.0
Sn-1.0Ag-0.6Zn	220.5	218.4	2.1

In addition, the DSC result of Zn doped solders in Table 3 indicates that Sn-Ag-Zn has a very small undercooling of about 2~3 °C, while Sn-1.0Ag has a large undercooling, about 30 °C. This is consistent with the result reported by Cho et al [13] that the minor elements having a hcp crystal structure such as Zn, Co, Mg, Ti, Sc, and Zr are very effective to reduce the undercooling of Sn. A small undercooling can promote easy nucleation and growth of β -Sn at a high temperature and increase the possibility to form large cyclic twins as a stable grain orientation of β -Sn may be less interrupted by growing IMC particles during cooling.

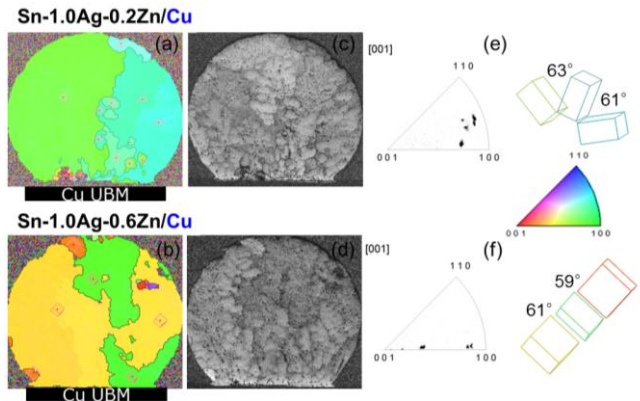


Figure 10. EBSD results of Sn-Ag-Zn/Cu UBM joints; (a) and (b), inverse pole figure maps; (c) and (d), image quality maps; and (e) and (f); inverse pole figures.

In Sn-Ag-Zn/Cu joints, fine twins near the joint interface or the large primary phase noticed in the Sn-Ag-Ni/Cu joints are not observed. Three or four large cyclic twins having 60 degree orientations are observed as shown in the EBSD result, Fig 10. The Cu dissolution in Sn-Ag-Zn promotes more the eutectic microstructure as well as large cyclic twins.

Microhardness

It has been reported that the microhardness of Sn-rich solders, Sn-Ag or Sn-Cu is strongly influenced by their microstructure, composition, solute content, and IMC characteristics (density, size and distribution) [8, 10]. It was also discussed a higher hardness of the air-cooled Sn-Ag over the quenched Sn-Ag was due to its high solubility of Ag in Sn compared to the Cu solubility. For the quenched Sn-Ag, most of Ag atoms would exist in a Sn solid solution, not contributing much to its hardness, while in the air-cooled Sn-Ag, most Ag atoms would precipitate out as Ag_3Sn IMC particles, increasing its hardness. Since Cu has a much less solubility than Ag in Sn, the quenched Sn-Cu was found to be always harder than the air-cooled [8]. In addition, the formation of fine twins does not contribute to increase its hardness as shown in the quenched condition of Sn-Ag having numerous fine twins.

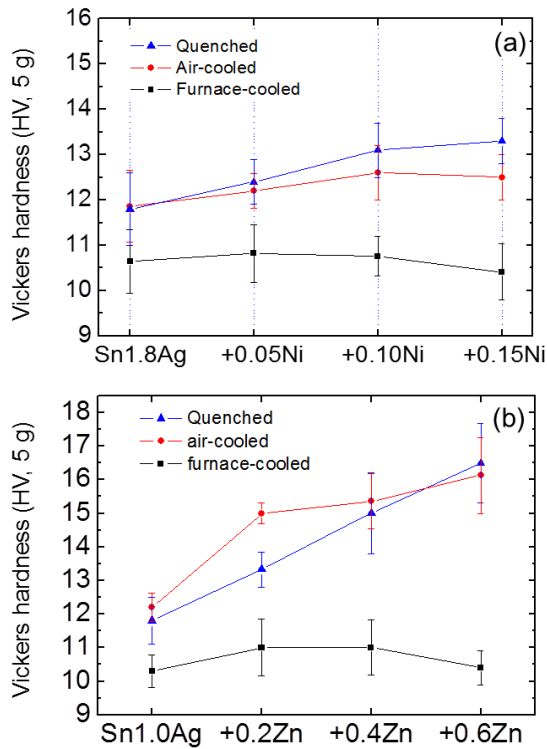


Figure 11. Vickers hardness data of (a) Sn-Ag-Ni and (b) Sn-Ag-Zn as a function of Ni or Zn composition and cooling rate.

Figure 11 displays the Vickers hardness data as functions of Ni or Zn composition and cooling rate. Ni or Zn addition to Sn-Ag increases the hardness of solders for the quenched or air-cooled condition, not in the furnace-cooled. As the alloying amount increases, the hardness increases in general. This is due to formation of various IMC particles; Ag_3Sn and

Ni_3Sn_4 in Sn-Ag-Ni, Ag_3Sn and $AgZn-\zeta$ in Sn-Ag-Zn. However, it is interesting to note that the effect of cooling rate is more influential to its hardening than the minor alloying addition of Ni or Zn to Sn. It is also remarkable to note some decrease in its hardness found with both Ni and Zn in the furnace-cooled solders. This may suggest that a small amount of Ni or Zn addition does not contribute to its solder hardening at all. This hardness reduction can be attributed to the microstructure coarsening, especially IMC coarsening in the furnace-cooled condition.

Summary

The minor alloying effects of Ni or Zn on the microstructure and microhardness of Pb-free solders are investigated in this study. The minor alloying addition of Ni or Zn to Sn-Ag solder significantly changes their microstructure and microhardness according to the quantity of alloying elements. The Ni addition of 0.15wt% to Sn-Ag leads to the drastic microstructure coarsening and reduces its undercooling less than 16 °C. The Zn addition from 0.2 to 0.6 wt% into Sn-Ag induces to form large cyclic twins even in the quenched cooling condition, differently from fine cyclic twins in Sn-Ag. Moreover, it is very effective to reduce the undercooling less than 3.5 °C. The microhardness of Sn-Ag-Ni and Sn-Ag-Zn solders are strongly affected by the alloying content, cooling rate, β -Sn dendrite size, grain size and IMC characteristics (type, density, and distribution).

References

1. S.K. Kang, D. Leonard, D.Y. Shih, L. Gignac, D.W. Henderson, S. Cho, J. Yu, "Interfacial reactions of Sn-Ag-Cu solders modified by minor Zn alloying addition," *J. Electron. Mater.*, Vol. 35, No. 3 (2006), pp. 479-485.
2. D. Kim, D. Suh, T. Millard, H. Kim, C. Kumar, M. Zhu, and Y. Xu, "Evaluation of high compliant low Ag solder alloys on OSP as a drop solution for the 2nd level Pb-free interconnection," *Proc 57th Electronic Components and Technology Conf*, Reno, NV, May 2007, pp. 1614-1619.
3. M.G. Cho, S. K. Kang, D. Y. Shih, and H. M. Lee, "Effects of Minor Additions of Zn on Interfacial Reactions of Sn-Ag-Cu and Sn-Cu Solders with Various Cu Substrates during Thermal Aging," *J. Electron. Mater.*, Vol. 36, No. 11 (2007), pp. 1501-1509.
4. T.R. Bieler, H. Jiang, L.P. Lehman, T. Kirkpatrick, and E. J. Cotts, "Influence of Sn Grain Size and Orientation on the Thermomechanical Response and Reliability of Pb-free Solder Joints," *Proc 56th Electronic Components and Technology Conf*, San Diego, CA, May 2006, pp. 1462-1467.
5. M. Lu, P. Lauro, D.-Y. Shih, P. Lauro, S. Kang, C. Goldsmith, S.-K. Seo, "The Effects of Ag, Cu Compositions and Zn Doping on the Electromigration Performance of Pb-Free Solders," *Proc 59th Electronic Components and Technology Conf*, San Diego, CA, May 2009, pp. 922-929.
6. S.-K. Seo, S.K. Kang, M.G. Cho, and H.M. Lee, "Electromigration Performance of Pb-free Solder Joints in

- terms of Solder Composition and Joint Path,” *JOM*, Vol. 62, No. 7 (2010), pp. 22-29.
7. S.-K. Seo, M.G. Cho, and H.M. Lee, “Crystal Orientation of β -Sn Grain in Ni(P)/Sn-0.5Cu/Cu and Ni(P)/Sn-1.8Ag/Cu Joints,” *J. Mater. Res.*, Vol. 25, No. 10 (2010), pp. 1950-1957.
 8. S.-K. Seo, S.K. Kang, D.-Y. Shih, and H.M. Lee, “An Investigation of Microstructure and Microhardness of Sn-Cu and Sn-Ag Solders as Functions of Alloy Composition and Cooling Rate,” *J. Electron. Mater.*, Vol. 38, No. 2 (2009), pp. 257-265.
 9. S.-K. Seo, S.K. Kang, D.-Y. Shih, and H.M. Lee, “The evolution of microstructure and microhardness of Sn–Ag and Sn–Cu solders during high temperature aging,” *Microelectron. Reliab.*, Vol. 49 (2009), pp. 288-295.
 10. M.G. Cho, S.K. Kang, S.-K. Seo, D.-Y. Shih, and H.M. Lee, “Interfacial Reactions and Microstructures of Sn-0.7Cu-xZn Solders with Ni-P UBM during Thermal Aging,” *J. Electron. Mater.*, Vol. 38, No. 11 (2009), pp. 2242-2250.
 11. S.-K. Seo, S.K. Kang, M.G. Cho, D.-Y. Shih, and H.M. Lee, “The Crystal Orientation of β -Sn Grains in Sn-Ag and Sn-Cu Solders Affected by Their Interfacial Reactions with Cu and Ni(P) Under Bump Metallurgy,” *J. Electron. Mater.*, Vol. 38, No. 12 (2009), pp. 2461-2469.
 12. J.Y. Tsai, Y.C. Hu, C.M. Tsai, and C.R. Kao, “A Study on the Reaction between Cu and Sn3.5Ag Solder Doped with Small Amounts of Ni,” *J. Electron. Mater.*, Vol. 32, No. 11 (2003), pp. 1203-1208.
 13. M.G. Cho, H.Y. Kim, S.-K. Seo, and H.M. Lee, “Enhancement of heterogeneous nucleation of β -Sn phases in Sn-rich solders by adding minor alloying elements with hexagonal closed packed structures,” *Appl. Phys. Lett.*, Vol. 95 (2009), 021905.